ACS Chemical Neuroscience

Letter

pubs.acs.org/chemneuro

Neoglucosylated Collagen Matrices Drive Neuronal Cells to Differentiate

Laura Russo,[†] Antonella Sgambato,[†] Marzia Lecchi,[†] Valentina Pastori,[†] Mario Raspanti,[‡] Antonino Natalello,[†] Silvia M. Doglia,[†] Francesco Nicotra,[†] and Laura Cipolla*[,†]

[†]Department of Biotechnology and Biosciences, University of Milano-Bicocca , P.zza della Scienza 2, I-20126 Milano, Italy

[‡]Department of Human Morphology, Human Morphology Laboratory, University of Insubria Via Monte Generoso 71, I- 21100 Varese, Italy

Supporting Information

ABSTRACT: Despite the relevance of carbohydrates as cues in eliciting specific biological responses, glycans have been rarely exploited in the study of neuronal physiology. We report thereby the study of the effect of neoglucosylated collagen matrices on neuroblastoma F11 cell line behavior. Morphological and functional analysis clearly showed that neoglucosylated collagen matrices were able to drive cells to differentiate. These data show for the first time that F11 cells can be driven from proliferation to differentiation without the use of chemical differentiating agents. Our work may offer to cell biologists new opportunities to study neuronal cell differentiation mechanisms in a cell environment closer to physiological conditions.

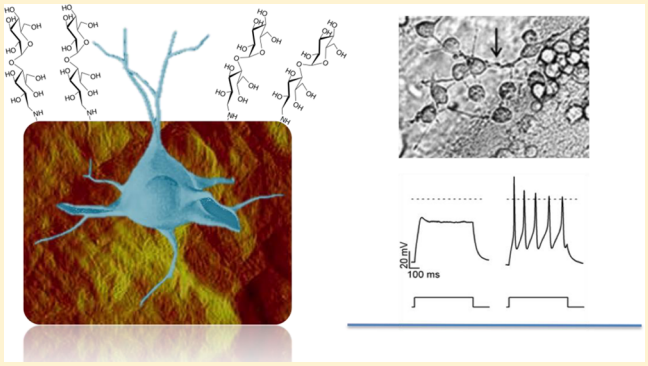

KEYWORDS: *Neuroblastoma F11 cell line, carbohydrates, collagen film, biomaterial*

Carbohydrates afford a versatile and powerful wealth to generate biochemical signals, the so-called "sugar code",[1] since they greatly exceed other classes of biomolecules in coding capacity. Despite their well recognized primary role in a variety of molecular recognition phenomena of biological relevance, glycans have been rarely exploited in the study of neuronal physiology and in tissue regeneration. In the nervous system, post-translational glycosylation has crucial roles in neurite outgrowth and in fasciculation, in synapse formation and modulation[2−5] in both the developing and mature nervous system.[6−8] Moreover, the search of nature-inspired cues able to increase the efficiency of synaptic connections is of outmost relevance in biomaterial design for nervous system regeneration.[9]

Thus, we prepared collagen matrices decorated with glucose moieties at their surface in order to investigate neuroblastoma F11 cell line behavior on grafted glucose. Collagen was chosen as the matrix since it is the main component of extracellular matrix (ECM), reported as a good biocompatible substrate for in vitro cell culture,[10,11] and widely used in the clinics as biomaterial for regenerative medicine.[12] Collagen is usually glycosylated with α-(1→2)-D-glucosyl-β-D-galactosides linked to hydroxylysine residues, where glucose is added as the last residue and most likely elicits a specific biological response. For this reason, we decided to investigate the effect of collagen matrix neoglucosylation on neuronal differentiation.

Collagen Type I from bovine Achilles tendon was used for the preparation of two-dimensional (2D) scaffold by a solvent casting method.[11,13] Glucose decoration at the collagen surface was achieved by reacting lysine side-chain amino groups with 0.06 M maltose aq. solution in 0.03 M $NaCNBH_3$ in citrate buffer (pH 6.00), leading to a covalent stable neoglycosylation in which an α-glucoside residue is correctly exposed for the interaction with the receptors (Figure 1a). The reaction can be extended to other reducing di- or polysaccharides to exploit the sugar diversity asset. To assess if the chemical treatment had any detrimental effect on supramolecular structure of neoglycosylated collagen, pristine collagen and the neoglycosylated collagen scaffolds were characterized by Fourier transform infrared (FTIR) spectroscopy in attenuated total reflection (ATR) mode and by atomic force microscopy (AFM) analysis, as reported in Figure 1b, d, and e. Intact collagen scaffolds displayed almost superimposable IR spectra also in the amide I band, which is due to the C═O stretching vibrations of the peptide bond. This result indicates the maintenance of the overall protein secondary structures after sample treatments. The analyses of the external layers of the collagen scaffold confirmed the success of the neoglycosylation reaction as indicated by the raising of the carbohydrate marker bands,[14,15] in the 1200−900 cm^{-1} region, only in the case of the treated sample.

The effectiveness of collagen neoglycosylation was determined by ^1H NMR spectroscopy, using maleic anhydride for

Published: March 13, 2014

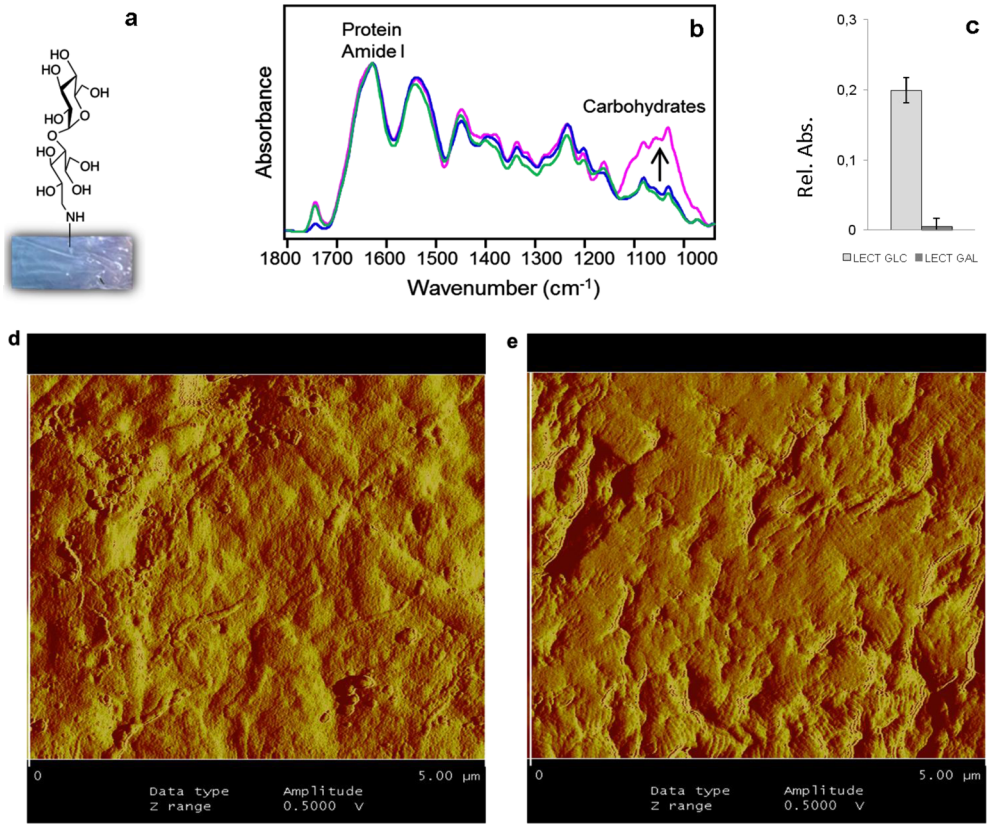

Figure 1. Structure and characterizations of the collagen matrices. (a) Neoglycosylated collagen scaffold. (b) FTIR absorption spectra of intact pristine (green line) and neoglycosylated (blue line) collagen and external layers (pink line) of the neoglycosylated collagen sample. (c) ELLA analysis. (d) AFM micrograph of native and (e) neoglycosylated collagen.

the quantification of residual lysine amino groups: roughly 20 nmol of saccharide/cm^2 have been added by reductive amination.

In order to assess if the exposed glucose residues could also exploit their biological signaling functions upon recognition of its complementary receptor, enzyme linked lectin assays (ELLAs)[16] were performed on the neoglycosylated collagen samples (Figure 1c). Commercially available peroxidase-conjugated lectins were used for the recognition of the surface-bound carbohydrate. Thus, Concanavalin-A (ConA) has been selected based on its ability to recognize α-glucosides, while peanut agglutinin (PNA) recognizing β-galactosides has been selected as negative control. The data in Figure 1c indicate the effective recognition of exposed α-glucoside by the complementary lectin. The observed absorbance values clearly indicate not only the presence but also the correct exposition of the saccharidic epitope on collagen surfaces.

Finally, a morphological evaluation of the collagen scaffold structure was carried out by AFM analysis. Small fragments of collagen scaffolds were mounted on appropriate stubs and observed with a Digital Instruments MultiMode Scanning Probe Microscope with a Nanoscope IIIa controller and a phase Extender, fitted with Nanosensors TESP silicon probes ($k \approx 42$ N m^{-1} and $f \approx 300$ kHz). All images were taken in Tapping-Mode AFM at 512 × 512 pixel with a fast axis scan speed of 1.5 − 2 Hz. Pristine collagen scaffold (Figure 1d) exhibited a mottled, finely granular surface interspersed with occasional fibrous structures. Neoglycosylated collagen scaffold highlights a greater tendency to form ordered structures, and its patch shows a number of short cross-banded segments randomly oriented (Figure 1e), which are similar to short stretches of native fibrils. A longitudinal striation, corresponding to the layout of the molecules, was also evident within the banded segments. This is a clear indication that the neoglycosylation process does not alter the size and the shape of the collagen molecules, which are still able to form ordered banded structures.

We then compared the behavior of neuroblastoma F11 cells[17] plated on pristine and neoglucosylated collagen with cells seeded on Petri dishes. We first observed that both native and neoglucosylated collagen did not have any detrimental effect on cell viability, thus demonstrating that the neoglycosylation did not affect the biocompatibility of the matrices. After 7 days, morphological and functional analysis of the three conditions were performed. Images at the confocal microscope revealed a significantly higher frequency of cells with neuritic-like processes when plated on neoglucosylated collagen (glc-collagen) compared to pristine collagen and Petri dishes (Figure 2a, b and Supporting Information Figure S1). Immunofluorescent staining with antibodies to the late neuronal marker β-tubulin confirmed that cells maintained for 7 days on glc-collagen were mature neurons (Figure 2c).

Neurite outgrowth may be a morphologic manifestation of differentiation.[18,19] Therefore, we decided to verify the acquisition of specialized neuronal properties by functional analysis. The electrophysiological properties of cells were analyzed by the patch-clamp technique in the whole-cell configuration. Voltage protocols were applied to measure sodium (I_{Na}) and potassium (I_K) current amplitudes and to compare current densities (Figure 2d). Na^+ current densities

dx.doi.org/10.1021/cn400222s | ACS Chem. Neurosci. 2014, 5, 261−265

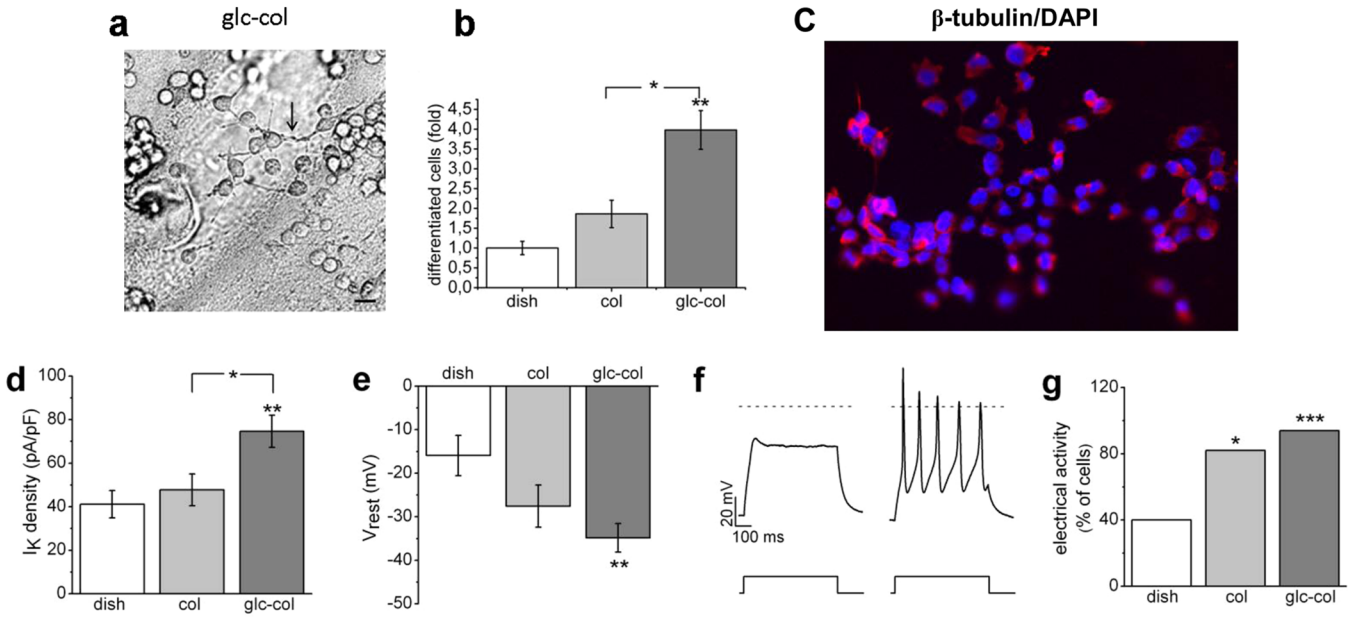

Figure 2. Morphological and electrophysiological properties of F11 cells maintained for 7 days on Petri dishes (dish), on pristine collagen (col), and on neoglycosylated collagen (glc-col). (a) Transmission image of F11 cells grown on neoglycosylated collagen: neuritic-like processes are indicated with an arrow; scale bar 30 μm. (b) Differentiated cell numbers, expressed in fold, relative to cells on Petri dishes. A significant difference was observed in cells plated on glc-col versus cells plated on Petri dishes (**$p < 0.01$) and versus cells plated on collagen (*$p < 0.05$). (c) Immunofluorescence of F11 grown on neoglycosylated collagen: β-tubulinIII antibody indentified neurons (red) and DAPI evidenced nuclei (blue). (d) Mean current density through potassium channels. A significant increase in the mean values was observed in cells plated on glc-collagen versus cells plated both on Petri dishes (**$p < 0.01$) and on pristine collagen (*$p < 0.05$). (e) Mean resting membrane potential for cells in the three conditions. Compared to cells plated on Petri dishes, a hyperpolarizing trend was evident for cells plated on pristine collagen and a significant difference was even obtained for cells plated on glc-col (**$p < 0.01$). (f) Representative response induced by a step current of 50 pA from a cell on the dish (left) and a cell on glc-collagen (right). The depolarizing current elicited a passive response in the cell on the dish, but triggered action potentials in the cell on glc-col. The action potential amplitude and duration is characteristic of differentiated F11 cells. The dot line in the traces represent the level of 0 mV. The current protocol is represented below the trace; holding potential, −75/−77 mV. (g) Percentage of cells endowed with electrical activity. Significantly higher values observed for both collagen (*$p < 0.05$) and glc-col (***$p < 0.001$).

showed the tendency to increase from Petri dishes (47.3 ± 18.8 pA/pF, n = 15), to collagen (81.4 ± 21.8 pA/pF, n = 12) and to neoglycosylated collagen (91.5 ± 13.9 pA/pF, n = 17); moreover, a significant higher mean I_K density was calculated for cells plated on neoglycosylated collagen (74.6 ± 7.4 pA/pF) compared to both Petri dishes (41.1 ± 6.3 pA/pF) and collagen (47.7 ± 7.3 pA/pF). Current recordings in voltage-clamp mode suggested that collagen matrices favored the expression of sodium and/or potassium channels in cell membranes and this was more evident for the neoglycosylated matrix.

Switching the system to the current-clamp mode, we measured the resting membrane potential (V_{rest}) and we monitored the electrical activity. Mean V_{rest} manifested very depolarized values in cells from the Petri dish (−15.9 ± 4.6 mV, n = 15) but showed a trend to hyperpolarize in collagen-plated cells (−27.5 ± 4.9 mV, n = 11) and was significantly more negative in glycosylated collagen-plated cells (−34.8 ± 3.3 mV, n = 18, $p < 0.01$) (Figure 2e). The electrical activity was tested by applying depolarizing current pulses by the patch-electrode (Figure 2f). In Petri dishes, the majority of the cells showed slow depolarisations which were not able to reach 0 mV, whereas mature action potentials (APs) were registered in 40% of cells. On the contrary, the fraction of cells able to generate APs was higher on collagen (82%) and reached almost the totality (94%) on neoglycosylated collagen (Figure 2g). These differences were significant for collagen ($p < 0.05$, χ^2 test) and highly significant for the neoglycosylated collagen ($p < 0.001$, χ^2 test). Overall, we observed that cells maintained on collagen matrices showed a more differentiated phenotype compared to cells plated on Petri dishes, and this was supported by morphological and physiological evidence: increasing frequency of cells with neuritic-like processes, higher sodium and potassium current densities, more hyperpolarized mean V_{rest}, and major probability to generate mature overshooting action potentials. Moreover, we observed that differentiating pressure provided by the neoglucosylated collagen matrix was the most pronounced. This observation shows for the first time that F11 cells can be driven from proliferation to differentiation without the use of chemical differentiating agents.[20,21]

Glycosylated proteins of the extracellular matrix are specifically recognized by cell surface proteins which are lectins or which contain characteristic lectin-domains.[22] Lectin-like proteins have been identified on the surface of a neuroblastoma cell line, associated with many proteins in high molecular weight complexes, and one of them, calreticulin, was found to be essential for adhesion and neurite formation.[23] Other cellular receptors for extracellular matrix components have been shown to trigger signaling pathways for migration, proliferation, survival, and differentiation by modulating ion channel properties. Some types of integrins have been shown to specifically activate a member of a potassium channel family, resulting in the control of neurite extension in neuroblastoma cells.[24,25] These observations suggest that glycosylated collagen might activate a signal pathway in which the activation of ion channels seems to represent a key step toward differentiation.

dx.doi.org/10.1021/cn400222s | ACS Chem. Neurosci. 2014, 5, 261−265

In conclusion, morphological and functional analysis showed that neoglucosylated collagen matrices were able to drive cells to differentiate without the use of chemical differentiating agents. This work may offer to cell biologists new opportunities to study neuronal cell differentiation mechanisms in a cell environment closer to natural conditions. Finally, the data presented in this report reinforce the idea that glycobiology represents an important tool of enlightenment for cellular and molecular medicine and for tissue repair processes.

METHODS

Collagen Preparation. Type I collagen films from bovine Achilles tendon (Sigma-Aldrich, catalog no. C9879) were produced by a solvent-casting method as previously described. Briefly, the collagen was dissolved in acetic acid 0.5 M for 4 h at 40 °C. The suspension was homogenized with a mixer for 2 min at maximum speed. After removal of the aggregates, 40 mL of collagen solution was poured into a 8.5 × 12.5 cm^2 culture multiwell lid and the solvent evaporated in the fume hood for 2 days. The collagen matrices were produced as thin transparent films (1 mg/cm^2), prepared as previously described.[11]

Collagen Neoglycosylation. A piece of collagen patch (80 mg, 12 cm × 7 cm) was immersed in 20 mL of 0.06 M maltose solution followed by the sequential addition of 0.03 M $NaBH_3CN$ in citrate buffer (pH 6.00) and reacted overnight. After this time, the collagen film was thoroughly washed first with 20 mL of milliQ (mQ) H_2O three times for 20 min, and finally with 20 mL of ethanol for 20 min.

Neoglycosylated Collagen Matrices Characterization. *NMR Quantification.* Derivatization of the native and neoglycosylated collagen samples with maleic anhydride was performed to label and quantify $-NH_2$ groups of lysine residues. Collagen films (32 mg) were immersed in a THF solution (0.04 M) of maleic anhydride in the presence of $NaHCO_3$. The reaction was carried out at room temperature overnight. After thoroughly washing with mQ H_2O, followed by ethanol, collagen films were dried under vacuum and then dissolved in 0.6 mL of 2 M NaOD in D_2O. ^1H NMR spectra were recorded using a Varian 400 MHz Mercury instrument, operating at a proton frequency equal to 400 MHz, at room temperature. The 90° pulse-width (pw90) was calibrated, the number of scans varied depending on the signal-to-noise ratio, and the recycling delay was 5 s.

Atomic Force Microscopy (AFM). Specimens obtained as above were dehydrated with increasing concentrations of ethanol and then with hexamethyldisilazane (HMDS, Sigma), immobilized onto biadhesive tape and observed with a Digital Instruments Multi-Mode Nanoscope IIIa equipped with a Digital Instruments phase Extender and fitted with Nanosensors Tesp-SS or with Olympus OTESPA silicon probes ($k \approx 42$ N m^{-1} and $f \approx 300$ kHz, for both). Images were obtained via tapping-mode atomic force microscopy in air, at a scan speed of 1.5−2 Hz, and at a resolution of 512 × 512 pixel.

Fourier Transform Infrared (FTIR) Spectroscopy. FTIR spectra in attenuated total reflection (ATR) were collected by using the Golden Gate device (Specac) equipped with a single reflection diamond element. The Varian 670-IR spectrometer (Varian Australia Pty Ltd., AU) was used under the following conditions: 2 cm^{-1} spectral resolution, 25 kHz scan speed, 512 scan coadditions, triangular apodization and nitrogen-cooled mercury cadmium telluride detector. A qualitative ATR/FTIR characterization of the surface of the collagen patches was obtained by scraping out their external layers on the ATR element and collecting the spectra of the materials moved out from the film. The absorption spectra were reported after baseline correction between 1800 and 900 cm^{-1} and normalization at the amide I band intensity to compensate for the different protein content.

Biological Assays. *ELLA Assays (Enzyme Linked Lectin Assay).* Pristine collagen and neoglycosylated collagen samples (1 × 1 cm^2, 1 mg) were blocked with a solution of 2% BSA in PBS (100 μL) and shaken (14 h, 5 °C), according to the manufacturer's protocol. The films were then removed and incubated at room temperature with a solution of Concanavalin-A from *Canavalia ensiformis* (Jack bean) peroxidase conjugate (Sigma-Aldrich, catalog no. L6397) (0.01 mg/mL, 200 μL) in PBS for 2 h under shaking. The films were then thoroughly washed with PBS to remove unbound lectins and then treated with a solution of OPD (SIGMAFAST OPD, Sigma-Aldrich, catalog no. P9187) (500 μL, 1 h). The absorbance of an aliquot of this solution (200 μL) was measured at 450 nm. Negative control has been performed adopting the same protocol using a solution of the lectin from *Arachis hypogaea* (peanut) peroxidase conjugate (Sigma-Aldrich, catalog no. L7759).

Cell Cultures. F11 cells (mouse neuroblastoma N18TG-2 x rat DRG[17]) were seeded on native and functionalized collagen patches at 60 000 cells/35 mm dish and were maintained without splitting until the day of the experiment. They were cultured in Dulbecco's modified Eagle's medium (Sigma-Aldrich), 10% of fetal calf serum (Sigma-Aldrich), 2 mM glutamine (Sigma-Aldrich) and incubated at 37 °C in a humidified atmosphere with 5% CO_2. They received fresh medium twice per week. Following a 7-day incubation period, the cells underwent morphological and functional analysis.

Optical Microscopy. Transmission images of F11 cells on the collagen scaffolds were obtained by the laser scanning confocal microscope Leica Mod, TCS-SP2 (Leica Microsystems Heidelberg GmbH, Mannheim, Germany) coupled to a DMIRE2 inverted microscope, using the 20X objective HC PL FLUOTAR with N.A. of 0.5. Image processing was performed with Leica Confocal Software (LCS) and Adobe Photoshop Software. For each experiment 10 images were analyzed. No significant differences were observed in cell morphology between cells plated on native collagen and Petri dishes (Supporting Information Figure 1). However, visualization of cells maintained on native collagen was difficult due to collagen's ability to embed cells.

Immunofluorescence Analysis. F11 cells were seeded onto coverslips coated with neoglycosylated collagen patches (30 000 cells/coverslip) and grown for 7 days, receiving fresh medium twice per week. Cells were fixed for 20 min in 4% (w/v) paraformaldehyde in PBS and permeabilized by incubation in the presence of 0.3% (v/v) Triton-X100 for 90 min at room temperature. After blocking with 10% normal goat serum, cells were incubated overnight at 4 °C with anti-β-tubulinIII antibody (1:400, Covance, Princeton). After removal of the primary antibody and extensive washes with PBS, cells were incubated at room temperature for 45 min with a secondary antibody labeled with Alexa Fluor 546 (1:800, Molecular Probes). Samples were finally incubated for 10 min with DAPI (0.3 mg/mL, Roche Applied Science, Penzberg, Germany) for nuclear staining and rinsed with PBS for mounting and analysis. Microphotographs were taken using a Zeiss Axiovert 200 direct epifluorescence microscope (Zeiss Axioplan 2, Germany).

Patch-Clamp Recordings. Electrophysiological recordings were performed by the patch-clamp technique in the whole-cell configuration. The standard extracellular solution was bath applied and contained the following (mM): NaCl 135, KCl 2, $CaCl_2$ 2, $MgCl_2$ 2, hepes 10, glucose 5, pH 7.4. The standard pipet solution contained the following (mM): potassium aspartate 130, NaCl 10, $MgCl_2$ 2, $CaCl_2$ 1.3, EGTA 10, hepes 10, pH 7.3. Recordings were acquired by the pClamp8.2 software and the MultiClamp 700A amplifier (Axon Instruments), in the voltage-clamp or current-clamp mode. The information we extracted from the experiments were represented by sodium and potassium current densities, the resting membrane potential (V_{rest}), and the presence of action potentials evoked by depolarizing currents. Sodium and potassium currents were recorded by applying a standard protocol: starting from a holding potential of −60 mV, cells were conditioned at −90 mV for 500 ms and successively tested by depolarizing potentials in 10 mV increments, from −80 to +40 mV. Series resistance errors were compensated for to a level of up to 85−90%. The electrical activity was evoked by hyperpolarizing the V_{rest} at approximately −75 mV and by subsequently depolarizing with 600 ms long current pulses. The depolarization peaks were considered action potentials when they were higher than 0 mV. For the analysis, Origin 8 (Microcal Inc., Northampton, MA) and Excel were routinely used. Data are presented as mean ± SEM. Statistical evaluations were obtained using the one-way analysis of variance (ANOVA), followed by the Tukey post hoc test, and the χ^2 test.

■ ASSOCIATED CONTENT

Supporting Information

Figure S1. Transmission images of F11 cells. This material is available free of charge via the Internet at http://pubs.acs.org.

■ AUTHOR INFORMATION

Corresponding Author

*E-mail: e-mail:laura.cipolla@unimib.it.

Author Contributions

L.R., A.S., M.L., V.P., M.R., and A.N. performed the research; S.M.D., F.N., and L.C. looked for financial support for the project; all the authors contributed to the writing of the paper; L.R. designed the research.

Funding

We gratefully acknowledge Fondazione Cariplo, Grant No. 2010-0378, No. 2011-0270 and MIUR, under project PRIN 2010/L9SH3K.

Notes

The authors declare no competing financial interest.

■ ACKNOWLEDGMENTS

We thank Laura Rota Nodari for precious technical support with immunofluorescence analysis.

■ REFERENCES

(1) Gabius, H. J., Siebert, H. C., André, S., Jiménez-Barbero, J., and Rüdiger, H. (2004) Chemical biology of the sugar code. *ChemBioChem 13*, 740−764.

(2) Schachner, M., and Martini, R. (1995) Glycans and the modulation of neural recognition molecule function. *Trends Neurosci. 18*, 183−191.

(3) Yamamoto, S., Oka, S., Inoue, M., Shimuta, M., Manabe, T., Takahashi, H., Miyamoto, M., Asano, M., Sakagami, J., Sudo, K., Iwakura, Y., Ono, K., and Kawasaki, T. (2002) Mice deficient in nervous system-specific carbohydrate epitope HNK-1 exhibit impaired synaptic plasticity and spatial learning. *J. Biol. Chem. 277*, 27227−27231.

(4) Kalovidouris, S. A., Gama, C. I., Lee, L. W., and Hsieh-Wilson, L. C. (2005) A role for fucose $\alpha(1-2)$ galactose carbohydrates in neuronal growth. *J. Am. Chem. Soc. 127*, 1340−1341.

(5) Kleene, R., and Schachner, M. (2004) Glycans and neural cell interactions. *Nat. Rev. Neurosci. 5*, 195−208.

(6) Dani, N., and Broadie, K. (2012) Glycosylated synaptomatrix regulation of trans-synaptic signaling. *Dev. Neurobiol. 72*, 2−21.

(7) Ohtsubo, K., and Marth, J. D. (2006) Glycosylation in cellular mechanisms of health and disease. *Cell 126*, 855−867.

(8) Langer, R., and Tirrell, D. A. (2004) Designing materials for biology and medicine. *Nature 428*, 487−492.

(9) Masand, S. N., Perron, I. J., Schachner, M., and Shreiber, D. I. (2012) Neural cell type-specific responses to glycomimetic functionalized collagen. *Biomaterials 33*, 790−797.

(10) Kothapalli, C. R., and Kamm, R. D. (2013) 3D matrix microenvironment for targeted differentiation of embryonic stem cells into neural and glial lineages. *Biomaterials 34*, 5995−6007.

(11) Taraballi, F., Zanini, S., Lupo, C., Panseri, S., Cunha, C., Riccardi, C., Marcacci, M., Campione, M., and Cipolla, L. (2013) Amino and carboxyl plasma functionalization of collagen films for tissue engineering applications. *J. Colloid Interface Sci. 394*, 590−597.

(12) Abou Neel, E. A., Bozec, L., Knowles, J. C., Syed, O., Mudera, V., Day, R., and Hyun, J. K. (2013) Collagen - Emerging collagen based therapies hit the patient. *Adv. Drug. Delivery Rev. 65*, 429−456.

(13) Tiller, J. C., Bonner, G., Pan, L. C., and Klibanov, A. M. (2001) Improving biomaterial properties of collagen films by chemical modification. *Biotechnol. Bioeng. 73*, 246−252.

(14) Natalello, A., Ami, D., Brocca, S., Lotti, M., and Doglia, S. M. (2005) Secondary structure, conformational stability and glycosylation of a recombinant Candida rugosa lipase studied by Fourier-transform infrared spectroscopy. *Biochem. J. 385*, 511−517.

(15) Guilbert, M., Said, G., Happillon, T., Untereiner, V., Garnotel, R., Jeannesson, P., and Sockalingum, G. D. (2013) Probing non-enzymatic glycation of type I collagen: A novel approach using Raman and infrared biophotonic methods. *Biochim. Biophys. Acta 1830*, 3525−3531.

(16) Slaney, A. M., Wright, V. A., Meloncelli, P. J., Harris, K. D., West, L. J., Lowary, T. L., and Buriak, J. M. (2011) Biocompatible carbohydrate-functionalized stainless steel surfaces: a new method for passivating Biomedical Implants. *ACS Appl. Mater. Interfaces 3*, 1601−1612.

(17) Platika, D., Boulos, M. H., Baizer, L., and Fishman, M. C. (1985) Neuronal traits of clonal cell lines derived by fusion of dorsal root ganglia neurons with neuroblastoma cells. *Proc. Natl. Acad. Sci. U.S.A. 82*, 3499−3503.

(18) Edsjö, A., Holmquist, L., and Påhlman, S. (2007) Neuroblastoma as an experimental model for neuronal differentiation and hypoxia-induced tumor cell dedifferentiation. *Semin. Cancer. Biol. 17*, 248−256.

(19) Abemayor, E., and Sidellt, N. (1989) Human Neuroblastoma Cell Lines as Models for the In Vitro Study of Neoplastic and Neuronal Cell Differentiation. *Environ. Health Perspect. 80*, 3−15.

(20) Chiesa, N., Rosati, B., Arcangeli, A., Olivotto, M., and Wanke, E. (1997) A novel role for HERG K+ channels: spike-frequency adaptation. *J. Physiol. 501*, 313−318.

(21) Wieringa, P., Tonazzini, I., Micera, S., and Cecchini, M. T. (2012) Nanotopography induced contact guidance of the F11 cell line during neuronal differentiation: a neuronal model cell line for tissue scaffold development. *Nanotechnol. 23*, 275102−275116.

(22) McDonnell, J., Jones, G. E., White, T. K., and Tanzer, M. L. (1996) Calreticulin binding affinity for glycosylated laminin. *J. Biol. Chem. 271*, 7891−7894.

(23) Xiao, G., Chung, T. F., Pyun, H. Y., Fine, R. E., and Johnson, R. J. (1999) KDEL proteins are found on the surface of NG108−15 cells. *Mol. Brain Res. 72*, 121−128.

(24) Arcangeli, A., Becchetti, A., Mannini, A., Mugnai, G., De Filippi, P., Tarone, G., Del Bene, M. R., Barletta, E., Wanke, E., and Olivotto, M. (1993) Integrin-mediated Neurite Outgrowth in Neuroblastoma Cells Depends on the Activation of Potassium Channels. *J. Cell Biol. 122*, 1131−1143.

(25) Cherubini, A., Hofmann, G., Pillozzi, S., Guasti, L., Crociani, O., Cilia, E., Di Stefano, P., Degani, S., Balzi, M., Olivotto, M., Wanke, E., Becchetti, A., Defilippi, P., Wymore, R., and Arcangeli, A. (2005) Human *ether-a-go-go*-related Gene 1 Channels Are Physically Linked to β1 Integrins and Modulate Adhesion-dependent Signaling. *Mol. Biol. Cell 16*, 2972−2983.